Macromolecules
ARTICLE

Macromolecules **2010**, *43*, 9881–9891 **9881**
DOI: 10.1021/ma101682t

Direct Measurement of Polymer Chain Conformation in Well-Controlled Model Nanocomposites by Combining SANS and SAXS

Nicolas Jouault,[†,‡] Florent Dalmas,[§] Sylvère Said,[⊥] Emanuela Di Cola,[∥] Ralf Schweins,[○] Jacques Jestin,*[,†] and François Boué[†]

[†]*Laboratoire Léon Brillouin CEA/CNRS (LLB), CEA Saclay 91191 Gif-sur-Yvette Cedex, France,* [§]*Institut de Chimie et des Matériaux Paris-Est (ICMPE), UMR 7182 CNRS/Université Paris-Est, 2-8 rue Henri Dunant 94320 Thiais, France,* [⊥]*Laboratoire d'Ingénierie des Matériaux de Bretagne (LIMTAB), Université de Bretagne Sud (UBS), Centre de Recherche, Rue Saint Maudé, BP 92116, 56321 Lorient cedex, France,* [∥]*European Synchrotron Radiation Facility (ESRF), BP 220, 38043 Grenoble, France, and* [○]*Institut Laue Langevin (ILL) DS/LSS 6 rue Jules Horowitz, 38042 Grenoble Cedex 9, France.* [‡]*Present address: Laboratoire Matière et Systèmes Complexes (MSC), UMR 7057, Université Paris 7-Diderot, 75205 Paris cedex 13, France.*

Received July 26, 2010; Revised Manuscript Received September 17, 2010

ABSTRACT: We studied by small-angle neutron scattering (SANS) the polymer chain conformation in model silica/polystyrene (PS) nanocomposites. Using the zero average contrast method, we can properly match silica signal to directly measure the form factor of a single PS chain. An important effort has been put to eliminate the silica scattering using two distinct approaches (called respectively "three" and "four" components methods) leading to analogue results. By combining SANS data with small-angle X-ray scattering (SAXS) measurements and transmission electronic microscopy (TEM) images on the same samples, we obtain a very clear result about the effect on polymer chain conformation of the filler dispersion, either at low filler volume fraction, where silica arrange in small aggregates or at higher concentration where it forms a connected network. From SANS the chain conformation in nanocomposites is identical to the one without silica in a large q range illustrating that the chain conformation remains independent of the filler dispersion whatever the silica connectivity or the polymer molecular weight. This result opens the way to a better overview of the polymer chain conformation contribution, especially adsorption or chain mobility modification effects, in the complex mechanical reinforcement mechanisms of nanocomposites. However, at low q, an unexpected shoulder appears in the SANS curves: this effect does not vary in a systematic way neither with chain molecular weight nor with silica concentration. The non reproducibility of these observations could be related to unusual phase separation between normal and deuterated chains.

I. Introduction

The modification of polymer chains conformation at the local scale in constraint environments (porous media, thin films, nanocomposites, ...) can affect the macroscopic properties of materials (conductivity, glass transition temperature, mechanical properties, ...). In particular, polymer nanocomposites and their impressively improved mechanical properties compared to the pure matrix are very interesting materials for many applications.[1−3] A real fundamental understanding of the microscopic mechanisms involved here is still a challenging issue. Direct interactions between fillers are present and important, as seen from the important variations generated by different dispersions of the nanoparticles in the polymer matrix.[4] Polymer−filler interactions are also important, whether they are proposed to involve elastic contributions, through modification of the chain mobility at the vicinity of the filler inducing heterogeneities in the continuous polymer phase.[5,6] In all cases, knowing how much the chain conformation is modified in the presence of fillers could be key information from both fundamental and industrial point of view. Small-angle neutron scattering (SANS) has been shown to be the most suitable technique to shed a light on this class of systems, thanks to the specific contrast variation method which let match fillers to only measure the form factor of a single chain.

Although several works have been devoted to the chain conformation in pure polymer bulk by SANS,[7−9] the effect of geometrical constraints or confinement on chain conformation has been barely studied in the literature. Lal et al.[10] have reported on the effect of confinement on polystyrene polymers in glass channels (Vycor) and observed the reduction of the radius of gyration of confined chains compared to the equivalent in bulk, due to effects transverse to these channels. Contradictory is the observation by Nieh et al.[11] of an increase in chain dimension with increased confinement. Shin et al.[12] observed that the radius of gyration of the polymer in alumina nanopores is identical to that in the bulk over a wide range of molecular weights and pore diameters. Chain conformation was also investigated in thin films, since they showed much debated changes in their properties compared to bulk. Some experiments have revealed that chains dimensions are unaffected in parallel direction, but modified in normal direction, at least at intermediate scale depending on thin films thicknesses.[13] On the contrary, other authors did not observe any change in chain conformation.[14] All these observations on thin films or porous media show the controversial aspect of chain conformation in confined environments.

The case of nanocomposites is slightly different as it does not implicate especially a direct geometrical confinement of the chains as for the previous cases. Some numerical simulations provide different results for the chain arrangement depending on the nature of the system, the molecular weight of the polymer and the quality of filler dispersion.[15−18] Others studies at more local molecular scale on nanocomposites have been focused on the influence of fillers on structural and dynamical properties.

*Corresponding author. E-mail: jacques.jestin@cea.fr.

Published on Web 11/04/2010

Vacatello[19,20] studied model nanoparticles in short chains matrix, with variable nanoparticles size and volume fraction. For a nanoparticle size close to the one of the chains it has been observed that chains form coronas around nanoparticles with slow dynamic.[21] The global conformation is affected by the presence of nanoparticles with the radius of gyration reduced compared to the unfilled system. Nevertheless, these results need to be experimentally validated. As discussed above, direct structural information can be obtained by SANS, thanks to specific contrast-matching method; however, the literature reports also in this case contradictory results about the behavior of chain dimension with or without fillers.[22−26] One of the possible origins could be the uncertainties coming from the matching of the filler leading to an unambiguous measurement of the chain conformation. Nakatani et al.,[22] Mackay et al.[23] (for the C60/PS system) and also Botti et al.[24] extracted the conformation of the polymer chain from a complex scattering signal in which the interactions between labeled and nonlabeled chains have to be taken into account. Sen et al.[25] used the zero average contrast (ZAC) method, which cancels inter and intrachains correlations, but in unperfected matching conditions. The only unambiguous contrast matched method used is the one of Mackay et al.[26] with cross-linked PS particles as fillers but concerns a very specific case of nanocomposites filled with soft fillers. Another contribution for this debate could be that the results are system dependent. More precisely the structural arrangement of fillers in polymer matrix plays an important role. It has been reported that fillers can arrange in various dispersion according to preparation condition,[27,28] surface modification[29] which thus can lead to different chain conformations. Several results seem to depend on the characteristic size of the chain (R_g) and of the filler network (ξ) involved in the different systems. Nakatani et al.[22] observed a change in R_g as a function of filler volume fraction depending on chains sizes. For chain dimension comparable to the filler one, they observed a decrease of chain size for all filler concentrations. On the contrary for dimensions larger than those of the fillers, the chain size reaches a maximum: an increase at low filler concentrations followed by a decrease, reaching a dimension still larger than the unfilled polymer. From these results it appears that good dispersion is required for increase of radius of gyration[23,26] whereas others dispersion qualities,[25] from small aggregates to large agglomerates, induce no changes in chain conformation. However, this dispersion is not systematically characterized[22] leading to ambiguous influence of silica arrangement on chain conformation. These results suggest that it is fundamental to characterize properly the filler structure in polymer matrix from local to large scale in order to better understand the chain conformation.

In this context, we propose to investigate the polymer chain conformation in a classical model system, polystyrene (PS)/silica nanocomposites, extensively studied in the literature, which is representative of a large class of nanocomposites especially in term of filler dispersion and widely used for reinforcement. We propose to study the polymer chain conformation to see whether it will be affected by the presence of silica particles through adsorption, bridging effect or chain mobility modification induced by the filler organization as reported in the literature.[6,15] Relying on an accurate control of the nanocomposites processing conditions, we have combined small angle X-ray scattering (SAXS) and imaging (TEM) measurements to characterize the filler arrangements from the nano to the micro scale as a function of the filler volume fraction together with small angle neutron scattering (SANS) under special contrast conditions in order to directly measure the form factor of a single chain in the presence of fillers and access then to its conformation. We employed two different strategies of chain deuteriation in order to measure the single chain form factor inside the composite, namely the three and the four components methods. The second approach enables the validation, without any doubt, of the perfect matching of the silica fillers. Moreover, we have also investigated the chain SANS signal in a wide range of scattering vector q significantly extended toward the low q values region, corresponding to larger distances in the direct space.

The paper is organized as follows. First, we will present the zero average contrast method and describe the two different approaches employed in this work. Second, we will describe the silica structure by combining SAXS measurements and TEM images. Then we will focus on the chain conformation and study the influence of polymer molecular weight and silica volume fraction. Finally, we will compare our two methods and discuss in the last part the link between filler structure at the local scale and the chain conformation.

II. Material and Methods

II.1. Measurement of Chain Form Factor in Nanocomposites: Zero Average Contrast Method. The scattering intensity of a single chain in nanocomposite can be obtained directly by SANS using the zero average contrast (ZAC) method. This method was first used for a mix of normal, i.e., nondeuterated (H) and deuterated (D) chains in a solvent: the total scattering intensity $I(q)$ can be expressed by the relation 1:[30]

$$I(q) = (\rho_D - \rho_H)^2 x(1-x)\nu\Phi NP(q) + (x\rho_D + (1-x)\rho_H - \rho_0)^2[\nu\Phi NP(q) + V\Phi^2 S(q)] \quad (1)$$

where ρ_H, ρ_D, and ρ_0 are respectively the scattering length densities (SLD) of nondeuterated chains, deuterated chains, and solvent, x is the molar fraction of D-chains, ν is the molar volume of D monomer, V is the global volume, Φ is the molar fraction of polymer, $P(q)$ is the form factor of one chain, and $S(q)$ is the interchain structure factor. When the average contrast between polymer mix and solvent is adjusted to zero, i.e.:

$$(x\rho_D + (1-x)\rho_H - \rho_0 = 0) \quad (2)$$

The scattering intensity is only related to the form factor of one chain:

$$I(q) = (\rho_D - \rho_H)^2 x(1-x)\nu\Phi NP(q) \quad (3)$$

By this condition (eq 2), the intra and interchain correlations are matched and not observed. Equation 2 is possible when ρ_0 is comprised in between ρ_H and ρ_D; to meet this condition, mixtures of normal and deuterated solvents are often used. In our case, the role of the solvent is played by silica. The scattering length density has been determined by previous contrast variation experiments[31] in solvent and found to be equal to 3.41×10^{10} cm^{-2}. Some deviations from this value have been observed[25] depending on the density of the particles. For our particle, the matching composition to satisfy (2) is achieved by mixing 60.9% v/v hydrogenated (SLD of 1.41×10^{10} cm^{-2}) and 39.1% v/v deuterated (SLD of 6.53×10^{10} cm^{-2}) homopolymers. This first approach based on mixing silica with the H and D homopolymers only will be called three components method.

However, as will be discussed in the following, this method provides partially unexpected results. In order to fulfill the conditions of eq 2, we aimed at better matching by involving a fourth component method: a matrix made of statistical copolymer of normal (H) and deuterated (D) styrene with H/D proportion giving the same SLD of silica has been

synthesized. It is then mixed together with silica and the mix of H and D homopolymers. We called this second approach the four components ZAC method.

These two methods will be compared in the Results and Discussion sections.

II.2. Statistical Hydrogenated/Deuterated Copolymer. To ensure the perfect silica matching, we have synthesized a statistical H/D polystyrene whose scattering length density is equal to the silica scattering length density ($\rho = 3.41 \times 10^{10}$ cm^{-2}). To check the matching composition, contrast variation has been performed by varying the H/D ratio of statistic copolymer for different mixtures with silica. The statistical copolymers were synthesized by radical polymerization in solution by mixing normal styrene with deuterated styrene in an organic solvent (15% v/v of Dimethylacetamide DMAc) during 6 h at 80 °C. The polymer was precipitated in ethanol and filtrated to obtain a dry fibrous powder. The ratio H/D was modulated by varying normal styrene volume fraction from 35% to 100%. Table 1 presents the SLD of each synthesized copolymers.

Using each copolymer, nanocomposites filled with 5% v/v of silica were prepared and scattering intensities were measured by SANS. Figure 1a shows the evolution of scattering intensity as a function of the q wave vector for the different matrixes.

The scattering for different H/D ratio are compared with the complete hydrogenated case.

The scattering intensity at low q is decreasing by a factor 100 from the 100% hydrogenated curve to the one corresponding to the mixture of 65/35 H/D ratio. For this composition, the resulting signal coming from the silica particles is close to the background. Another representation is given in Figure 1 (b) by plotting the intensity at intermediate value of q ($q = 0.011$ Å^{-1}) as a function of the SLD of the copolymer matrix, assuming it has a H/D ratio equal to the one present in the styrene mixtures (no difference in chemical reactivity); it is again minimum for the 65/35 H/D ratio.

Molecular weight and weight distribution of the statistic copolymer were measured by size exclusion chromatography (GPC) giving a molecular weight M_n of 97800 g·mol^{-1} with polydispersity of $M_w/M_n = 1.74$, usual for such noncontrolled radical polymerization.

II.3. Nanocomposites Preparation. Nanocomposites were prepared according to the sample processing described in a former paper.[32] Nanocomposites were prepared by mixing nanosilica solution (Nissan-St, purchased by Nissan Chemical, with a mean radius of 6 nm and dispersed in dimethylacetamide, DMAc) with polymer solution (10% v/v in DMAc). For the first method (3 components), the polymer solution is composed of 60.9% v/v of H-PS and 39.1% v/v of D-PS provided by Polymer Source. Different molecular weights have been studied as listed in Table 2.

For the second method (4 components), the 10% polymer solution is composed of the matching matrix (75% in volume fraction), with 25% in volume fraction of a mixture of homopolymers, with 60.9% v/v of H−PS and 39.1% v/v of D−PS. Again they are provided by Polymer Source, and the different molecular weights are listed in Table 2.

In both cases the polymer−silica mixture is stirred for 2 h, then poured into Teflon molds and let cast in an oven at constant temperature (130 °C) during 8 days. As result, dry transparent films of dimension of 5 cm × 5 cm × 0.1 cm were obtained.

II.4. SANS and SAXS Measurements. *SANS.* Measurements were performed at the Laboratoire Léon Brillouin (LLB) on the SANS spectrometer PAXY and at the Institut Laue Langevin (ILL) on D11 spectrometer. Three configurations were used on PAXY: one with wavelength 12 Å, sample-to-detector distance of 6.70 m, and a collimation distance of 5.00 m, a second one with wavelength 6 Å, sample-to-detector distance of 6.7 m, and a collimation

Table 1. Normal Styrene Composition of the Different H/D Matrix with the Corresponding Scattering Length Densities (Calculated)

% normal styrene	calculated SLD ($\times 10^{10}$ cm^{-2})
35	4.732
45	4.22
50	3.963
55	3.708
65	3.196
67	3.094
80	2.43
100	1.41

Table 2. Molecular Weights and Polydispersity Index of all Normal (PS−H) and Deuterated (PS−D) Polystyrenes Used in This Study

PS−H		PS−D	
M_w (kg mol^{-1})	I_p	M_w (kg mol^{-1})	I_p
138	1.05	139.9	1.06
315	1.09	319	1.12
430	1.05	387	1.03
1777	1.3	2000	1.4

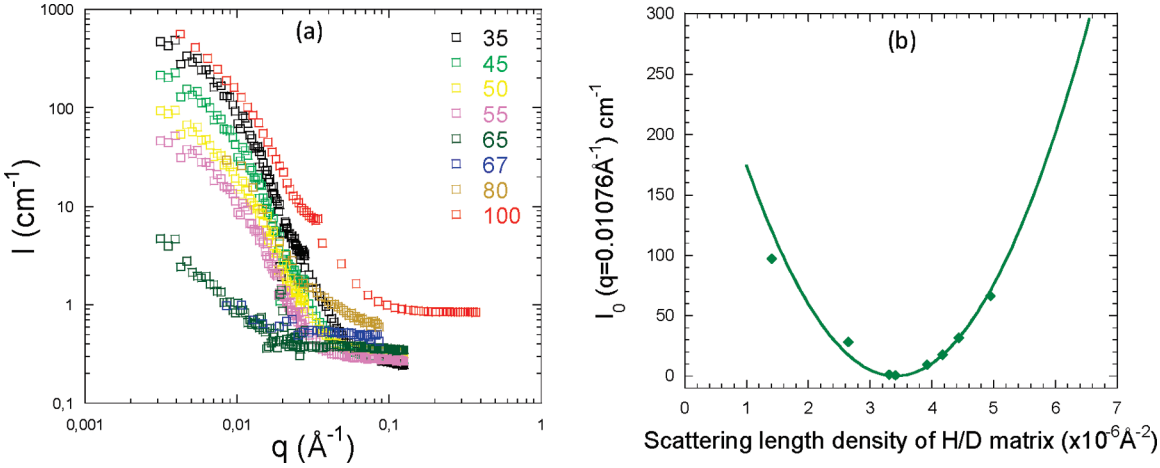

Figure 1. (a) SANS evolution of nanocomposites filled with 5% v/v of silica in different H/D matrixes. (b) SANS intensity at $q = 0.011$ Å^{-1} as a function of scattering length densities (SLD) of H/D matrixes. The match point is obtained for a 65/35 H/D ratio.

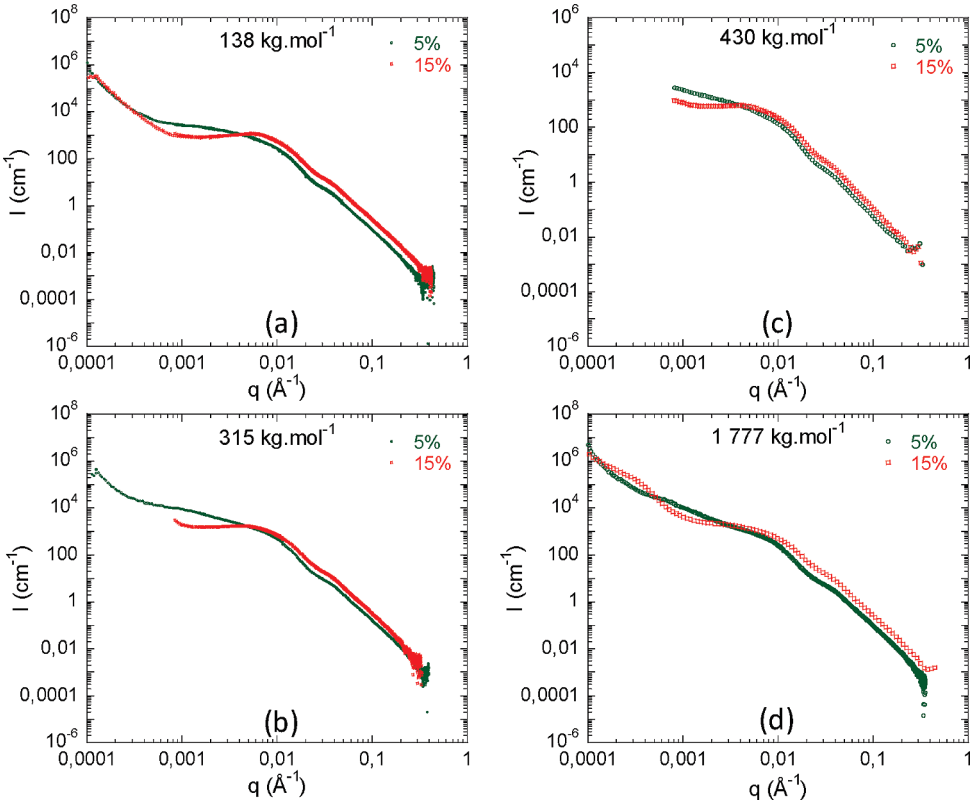

Figure 2. Influence of molecular weights of polymers on silica dispersion for the three components method. Scattering intensities (in cm^{-1}) obtained by SAXS measurements for nanocomposites filled with 5% v/v (green) and 15% v/v (red) for different molecular weights: (a) 138 kg mol^{-1}, (b) 315 kg mol^{-1}, (c) 430 kg mol^{-1}, and (d) 1777 kg mol^{-1}.

distance of 5.00 m, and the last one with wavelength 6 Å, sample-to-detector distance of 1.5 m, corresponding to a total q range of 2.5×10^{-3} to 0.25 $Å^{-1}$. On D11, three configurations were used: the first with a wavelength of 10 Å at a sample-to-detector distance of 34 m, the second at $\lambda =$ 6 Å at 8 mm and the third at $\lambda = 10$ Å at 2 m, providing an experimental q range of 0.0008 $Å^{-1} < q < 0.25$ $Å^{-1}$.

Data processing was performed with homemade programs following standard procedures with H_2O as calibration standard. Small deviations, found in the spectra at the overlap of two configurations, are due to different resolution conditions and (slight) remaining contributions of inelastic, incoherent, and multiple scattering. To get the cross-section per volume in absolute units (cm^{-1}), the incoherent scattering cross section of H_2O was used as a calibration. It was estimated from a measurement of the attenuator strength, and of the direct beam with the same attenuator. The incoherent scattering background subtraction is an important point. The incoherent scattering of nondeuterated and deuterated polymer was subtracted for the three components method, and for the four components method the H/D matrix incoherent scattering was measured and then subtracted.

SAXS. Small-angle X-ray scattering has been performed to investigate the filler dispersion in our nanocomposites. SAXS is not sensitive to the deuteriation process, and the contrast is only due to differences in electron densities of silica and polystyrene. The SAXS experiments were performed at the ESRF on ID-02 instrument using the pinhole camera at the energy of 12.46 keV at two sample-to-detector distances (1 and 10 m) corresponding to a q-range between 0.0008 $Å^{-1}$ and 0.3 $Å^{-1}$. The absolute units are obtained by normalizing respect to water (high q-range) or lupolen (low q-range) standard. In addition, for some samples, a Bonse-Hart camera setup was used, allowing one to reach a q-range lower than 0.0008 $Å^{-1}$.

II.5. Transmission Electronic Microscopy. The samples were cut at room temperature by ultramicrotomy using a Leica MZ6 Ultracup UCT microtome with a diamond knife. The cutting speed was set to 0.2 mm s^{-1}. The thin sections of about 40 nm thickness were floated on deionized water and collected on a 400-mesh copper grid. Transmission electron microscopy was performed on a FEI Tecnai F20 ST microscope (field-emission gun operated at 3.8 kV extraction voltage) operating at 200 kV. Precise scans of various regions of the sample were systematically done, from low to high magnification. The slabs observed were stable under the electron beam. The micrographs reported below are on average representative of the sample, which thus appears to be homogeneous.

III. Results

III.1. Silica Dispersion. In this part, we will focus on the silica structure in PS matrix in the two approaches (three and four components methods). Our aim was to characterize the filler arrangement at the local scale, in order to well identify under which conditions of filler spatial distribution we measure chain conformation, since we think it is critical. Silica dispersion has been investigated by coupling scattering SAXS and imaging TEM techniques which are both not sensitive to chain labeling.

III.1.1. Three Components Method. Figure 2 shows the scattering intensity of nanocomposites with different molecular weights (138 (a), 315 (b), 430 (c) and 1777 kg mol^{-1} (d)) for two silica volume fractions: 5% (green curves) and 15% (red curves) obtained by SAXS.

The filler dispersion on the model systems processed in exactly the same way has been described in a previous study.[32]

Independent of molecular weights or silica concentrations, at high q the scattering intensity decreases like q^{-4}, which is characteristic of a sharp interface between silica particles and polymer matrix. At intermediate q, a shoulder is observed at $q = 0.04$ Å^{-1}, which corresponds to the distance between primary particles in contact ($=2\pi/q$). At low q, different behaviors are observed depending on silica volume fraction. For 5%, a plateau is visible which is characteristic of finite-size objects. Experimental data can be fitted using form factor of aggregates; the fitting parameters are aggregation number N_{agg}, fractal dimension D_f and form factor of primary particles.[33] The results of the fits are presented in Table 3 for each molecular weight.

Table 3. Aggregation Numbers N_{agg} and Fractal Dimensions D_f of Aggregates for 5% Filled Nanocomposites for the Different Molecular Weights

M_w (kg mol^{-1})	N_{agg}	D_f
138	9	1.85
315	12	1.9
430	12	1.8
1777	10	1.85

The values are the same for each molecular weight (between 9 and 12 for N_{agg} and closed to 1.9 for D_f). TEM images in Figure 3 (on the left) confirm the results from SAXS investigations: primary particles arrange in small and open aggregates not directly connected.

At high silica volume fraction (15%), particles form a connected network and the values q* of peak position in SAXS curves give the mesh size $\xi = 2\pi/q^* \approx 70$ nm. These networks can be also observed in TEM micrographs which show good homogeneities in structure at larger scale. For $M_w = 1777$ kg mol^{-1}, no peak is observed but a plateau due to finite-size objects. A shoulder is observed at very low q corresponding to the signature of larger aggregates, clearly visible also on TEM images for the two silica concentrations. The presence of these large aggregates for large chains molecular weights can be explained by a decrease of entropy which can balance neither mixing enthalpy nor depletion effects, therefore enhancing the trend to demixtion between chains and particles. It is worth noting that all curves present an increase at very low q particularly highlighted by the measurements with the Bonse-Hart setup: we recognize a signal from crazes, created inside the sample during preparation process (drying and cooling below T_g).

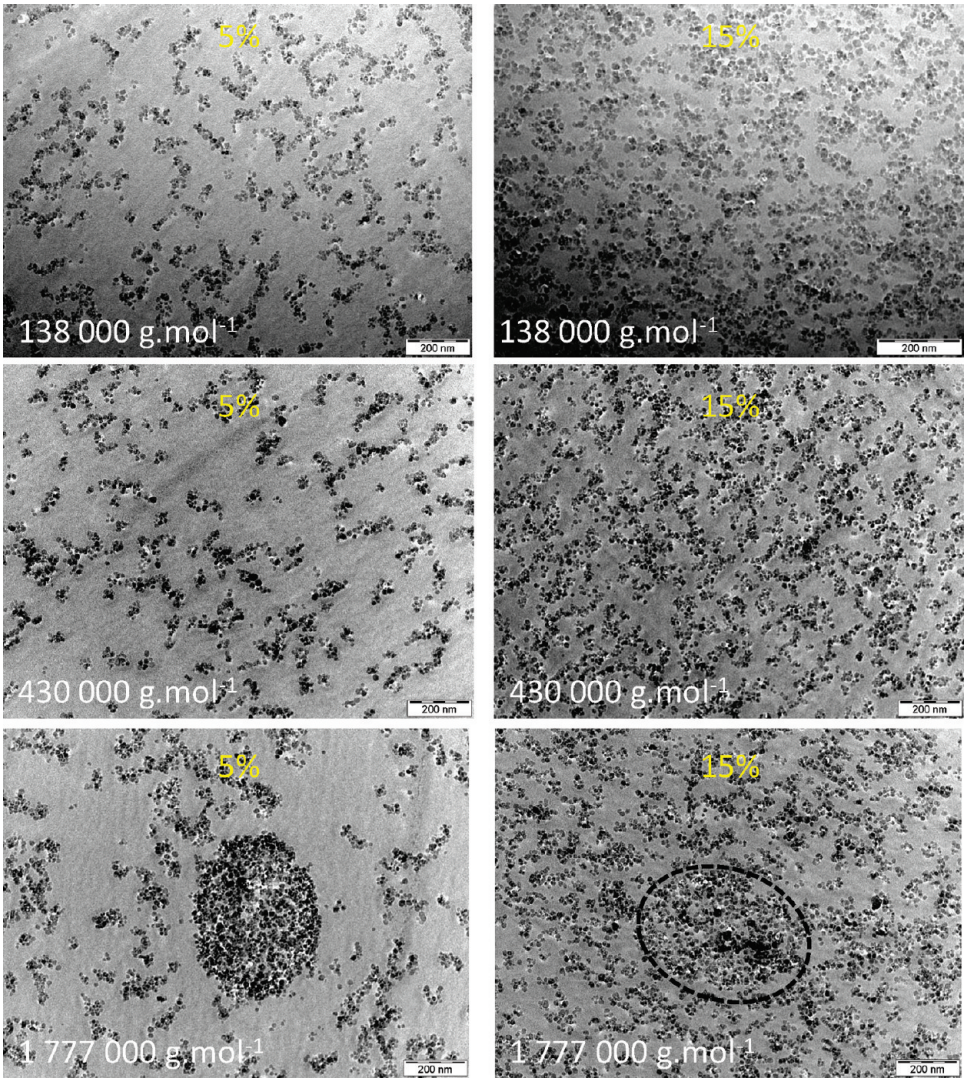

Figure 3. Transmission electronic microscopy (TEM) images on nanocomposites filled with 5% v/v (on the left) and 15% v/v (on the right) for different molecular weights. From the top to the bottom: 138 kg mol^{-1}, 430 kg mol^{-1}, and 1777 kg mol^{-1}. The dot circles for $M_w = 1777$ kg mol^{-1} are guide for the eyes to delimitate the large aggregates.

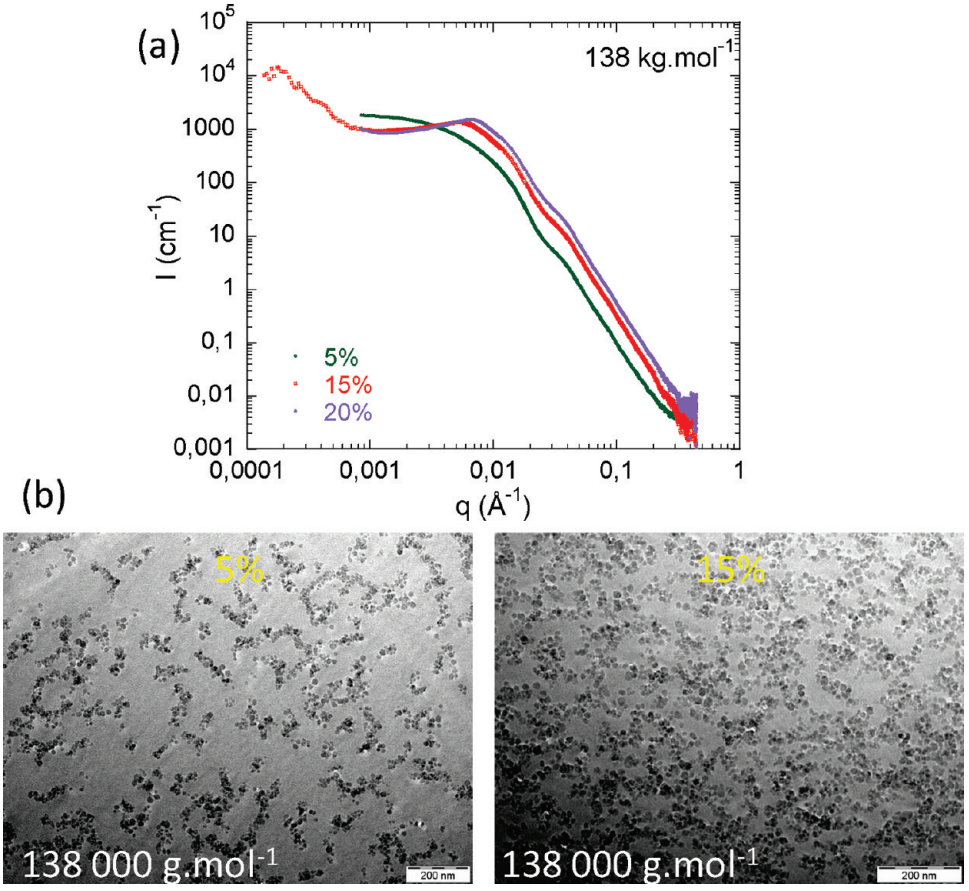

Figure 4. Silica dispersion for the four components method. (a) Scattering intensities from SAXS measurements for nanocomposites filled with 5% (green), 15% (red) and 20% v/v (purple). (b) TEM images for the nanocomposites filled with 5% (left) and 15% v/v (right).

III.1.2. Four Components Method. The same study has been done on samples prepared for the four components method.

Figure 4a shows SAXS results for $M_w = 138$ kg mol^{-1} as a function of silica volume fractions (5%, 15%, and 20% v/v) and Figure 4b shows the corresponding TEM images (for 5% on the left and 15% on the right). At low concentration the SAXS data are similar to the one described above for the three components method: primary particles form small aggregates at low concentration and filler network at higher silica volume fraction. At high concentration (15% v/v), the curve presents a correlation peak characteristic of a privileged distance between aggregates in the filler network, as also shown by TEM images. Whatever the matching method used, the samples show the same silica arrangement: hence we can use our results on chain conformation irrespectively of the matching method. In the following, investigation of chain conformation and the comparison between the two different approaches proposed will be reported.

III.2. Chain Conformation. Using the ZAC method in the presence of silica, we must be only sensitive to the form factor of a single chain.

III.2.1. The Unfilled Matrix. First, we report on the PS polymer without silica which will be used as reference.

For the three components method, Figure 5 presents SANS results for unfilled PS (blue circles) at various molecular weights from 138 to 1777 kg mol^{-1}.

For $M_w = 138$ to 430 kg mol^{-1}, the curves show the classical behavior of polymer chains with typical decrease at high q as q^{-2} (represented by a plateau at 0.11 cm^{-1} Å^{-2} in Iq^2 curves, as shown in the inset in Figure 5), and a plateau at low q in the Guinier regime which gives the radius of gyration of polymer chain. The curves can be described in the whole q range using the Debye equation[34] (eq 4) (red lines in Figure 5)

$$P(q) = \frac{2}{(q^2 R_g{}^2)^2}(e^{-q^2 R_g{}^2} - 1 + q^2 R_g{}^2) \qquad (4)$$

where $P(q)$ is the form factor of 1 chain and R_g its radius of gyration. Table 4 presents the values of radius of gyration for each molecular weight.

The radius of gyration of chain in polymer melt has been described in the literature and can be calculated by the following equation: $R_g = 0.275 M_w{}^{0.5}$. This gives for a molecular weight of $M_w = 138$ kg mol^{-1} a radius of gyration of 102 Å, for $M_w = 315$ kg mol^{-1}, R_g was found to be 154 Å, and for $M_w = 430$ kg mol^{-1}, $R_g = 180$ Å. These theoretical values are close to those obtained by fitting the Debye equation (see Table 4). The only deviation was observed in the case of $M_w = 1777$ kg mol^{-1}, for which theoretically a value of R_g of about 370 Å should be expected. However, SANS data show that for $M_w = 1777$ kg mol^{-1} the scattering intensity is in the low q region much larger than predicted by the Debye function, as highlighted in Figure 5d. The measured intensity (around 100000 cm^{-1}) is about 10 times larger than the predicted Debye one: this is characteristic of a spinodal decomposition of H−PS and D−PS mixture as predicted[9] and previously observed in the literature;[35−37] it will be discussed later in the text. For high molecular weights phase separation appears above a given D−PS volume fraction: this means this threshold is lower than $\Phi_{d\text{-}PS} = 0.4$ here, such that domains richer in D−PS are created. The domain growth is faster at a given scale, i.e., at a given q,

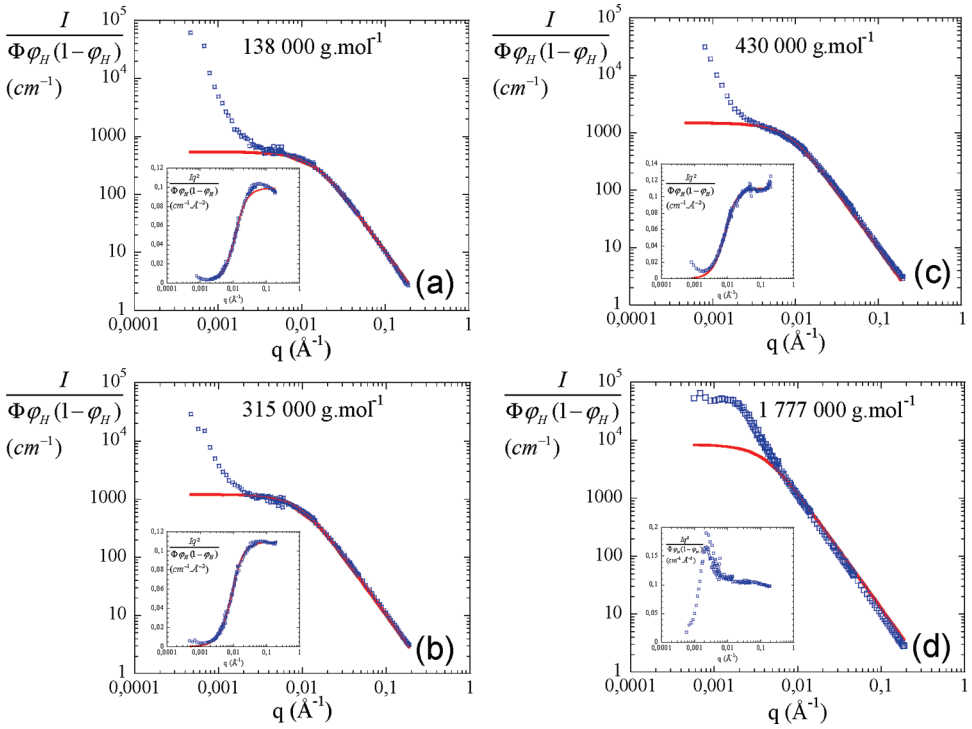

Figure 5. SANS signal of unfilled systems (reference) for different molecular weights: (a) 138 kg mol^{-1}, (b) 315 kg mol^{-1}, (c) 430 kg mol^{-1}, and (d) 1777 kg mol^{-1}. The red lines correspond to the fit using the Debye equation, eq 4. In the inset is shown the Kratky representation $Iq^2/\Phi\varphi_H(1-\varphi_H) = f(q)$.

Table 4. Values of Radius of Gyration for each Molecular Weight Obtained by the Debye Relation Eq 4

M_w (kg mol^{-1})	R_g (Å)
138	102
315	154
430	175

which results in a maximum in SANS curves giving a typical privileged size of the wormlike structure of those domains. At very low q, there is an upturn, where $I(q)$ scales as q^{-3} and which is again due to crazes. The presence of crazes is due to the contrast between the polymer and the vacuum, which is enhanced when the content in D segments is increased.

For the four components method, as previously discussed in the materials and methods part, the critical point is the correct subtraction of the background which corresponds to the scattering of H/D matrix and the incoherent scattering of D−PS and H−PS chains. The scattering intensity is given by the eq 5:

$$I(q) = I_{\text{total}} - [\Phi_{\text{H/D matrix}}(1-\Phi_{SiO_2})I_{\text{H/D matrix}} + \varphi_H I_{\text{inc-H}} + \varphi_D I_{\text{inc-D}}] \quad (5)$$

where I_{total} is the total scattering intensity, $\Phi_{\text{H/D matrix}}$ is the volume fraction of H/D matrix in the sample (=0.75), Φ_{SiO_2} is the silica volume fraction, $I_{\text{H/D matrix}}$ the scattering intensity of H/D matrix (measured alone), φ_H, φ_D and $I_{\text{inc-H}}$, $I_{\text{inc-D}}$, are respectively the volume fraction of H-chains (or D-chains) and $\varphi_H + \varphi_D = 0.25$) and the incoherent scattering of H-chains (or D-chains). Figure 7b shows the scattering intensity before subtraction of H/D matrix and incoherent of H and D chains. The increase at low q in H/D matrix is due to crazes not matched.

After this treatment we also obtained a classical curve for polymer chain (blue curve in Figure 7a discussed below) easily fitted by Debye equation with R_g = 105 Å close to the one measured in the three components method (102 Å).

III.2.2. Filled Systems: The Three Components Method. The results are presented in Figure 6 (with Kratky representations in insets). SANS data for filled systems reveal that, in the q-range between 0.01 and 0.25 Å^{-1}, the scattering intensities of filled polymers well superimpose with the unfilled one, whatever the molecular weights of the polymer or the silica volume fraction. The signal is unchanged and the presence of silica does not modify the chain form factor in this q range.

We consider now the larger molecular weight M_w = 1777 kg mol^{-1}. The scattering intensity of filled nanocomposites presents at low q a maximum similar to the one observed without silica (Figure 6d, green and red curves). This can be explained by demixing, in analogy with the case of the unfilled system. The maximum positions give the size of the domains which seem to be larger for the 5% than 15% volume fraction. This could mean that separation is slowed down when increasing confinement. At intermediate and high q (from 0.008 Å^{-1} to 0.2 Å^{-1}) the spinodal decomposition is not longer dominant anymore, as often observed in H/D homopolymer systems. In our case, the scattering intensity of filled systems scales as q^{-2} and superimposes with the reference one for the two silica concentrations. This suggests that even for these large chains, the single chain conformation is unchanged by the fillers which only affect separated domains.

We focus now on the other molecular weights: 138, 315, and 430 kg mol^{-1}. At glimpse, we can identify three different features depending on scale of observation. First, in the high and intermediate q the scattering intensities of filled nanocomposites scale as q^{-2} and superimpose well with the unfilled matrix signal. The presence of silica does not affect scattering intensities, therefore does not modify the chains form factor.

Our second observation extends on the whole q range: for molecular weight M_w = 315 kg mol^{-1} filled with 5% v/v

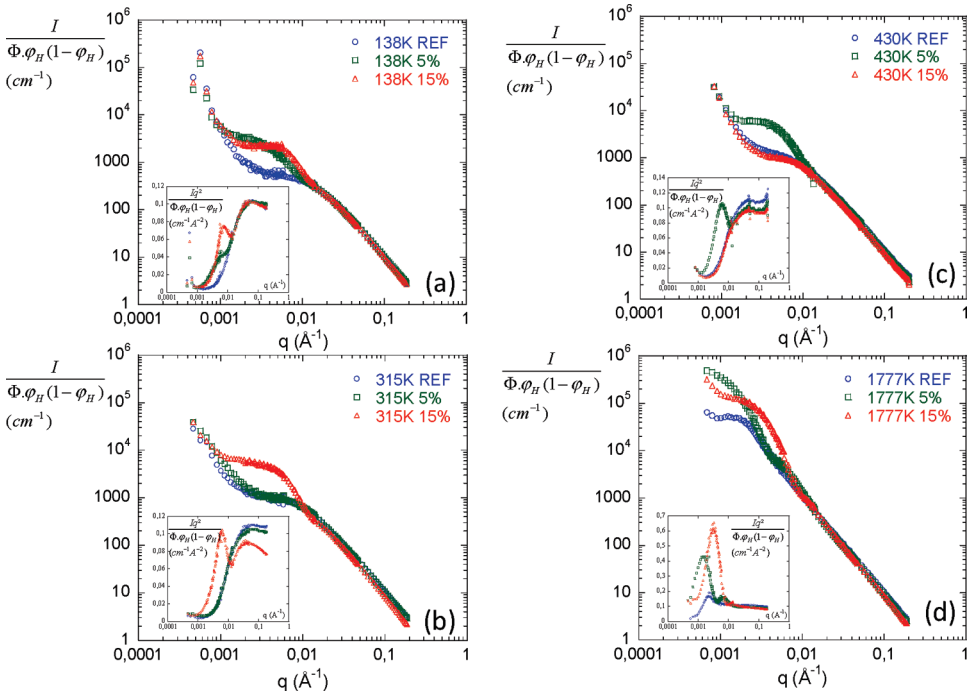

Figure 6. Scattering intensities normalized by $\Phi\varphi_H(1-\varphi_H)$ from SANS measurements for the three components methods for nanocomposites filled with 0% (blue circles), 5% (green squares) and 15% v/v (red triangles) at different molecular weights: (a) 138 kg mol^{-1}, (b) 315 kg mol^{-1}, (c) 430 kg mol^{-1}, and (d) 1777 kg mol^{-1}. In the inset is given the Kratky representation $Iq^2/\Phi\varphi_H(1-\varphi_H) = f(q)$.

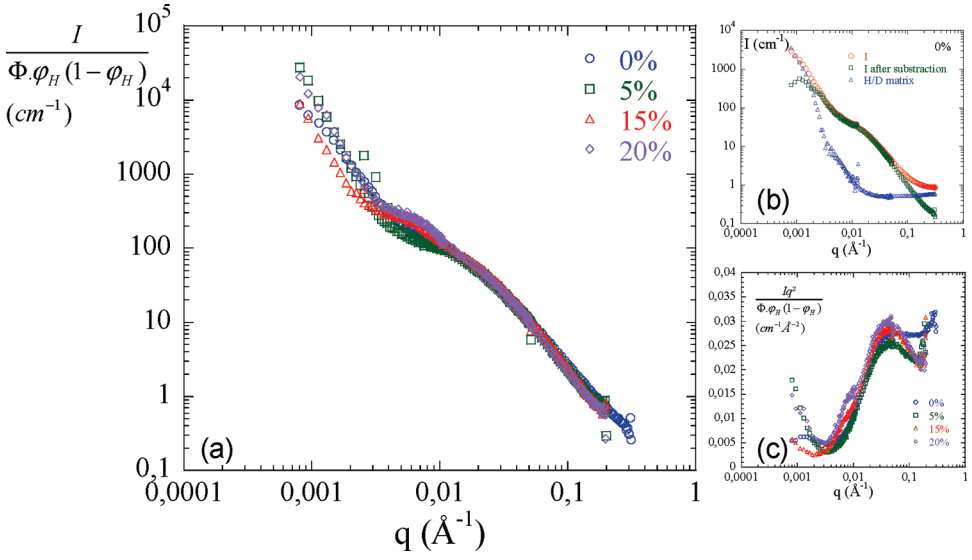

Figure 7. (a) Scattering intensities normalized by $\Phi\varphi_H(1-\varphi_H)$ from SANS measurements for the four components method for nanocomposites filled with 0% (blue circles), 5% (green squares), 15% (red triangles), and 20% v/v (purple diamonds) for a molecular weight of 138 kg mol^{-1}. (b) Scattering intensity before subtraction of H/D matrix signal (red circles) and after subtraction (green squares). (c) In the inset is shown the Kratky representation $Iq^2/\Phi\varphi_H(1-\varphi_H) = f(q)$.

and M_w = 430 kg mol^{-1} filled with 15% v/v, the scattering intensity superimposes well with the reference. SANS results clearly show that chain conformation is unperturbed by the presence of silica and independently of silica organization (small aggregates at 5% v/v or connected network at 15% v/v).

The third piece of evidence, however, is more puzzling: a shoulder appears in the scattering (in log−log representation) at low q, whose position seems independent of molecular weight and silica volume fractions. However, this phenomenon seems to be not reproducible: this shoulder appears according to an unsystematic way as a function of M_w. The shoulder is not observed at the same silica volume fractions for the different molecular weight: for 138 kg mol^{-1}, a shoulder is present both at 5% and 15% v/v, while for 315 kg mol^{-1} it is only at 15% v/v, and for 430 kg mol^{-1}, on the opposite, only at 5% v/v.

III.2.3. Filled Systems: the Four Components Method. Figure 7a (Iq^2 representations are shown in Figure 7c) shows the results for the molecular weight M_w = 138 kg mol^{-1} at different silica fractions using the four components method. Again, from 0.01 to 0.25 Å^{-1}, the superposition with unfilled is perfect, the scattering signal is not modified by the presence of silica: the chain form factor remains unchanged whatever the silica volume fractions. The very low

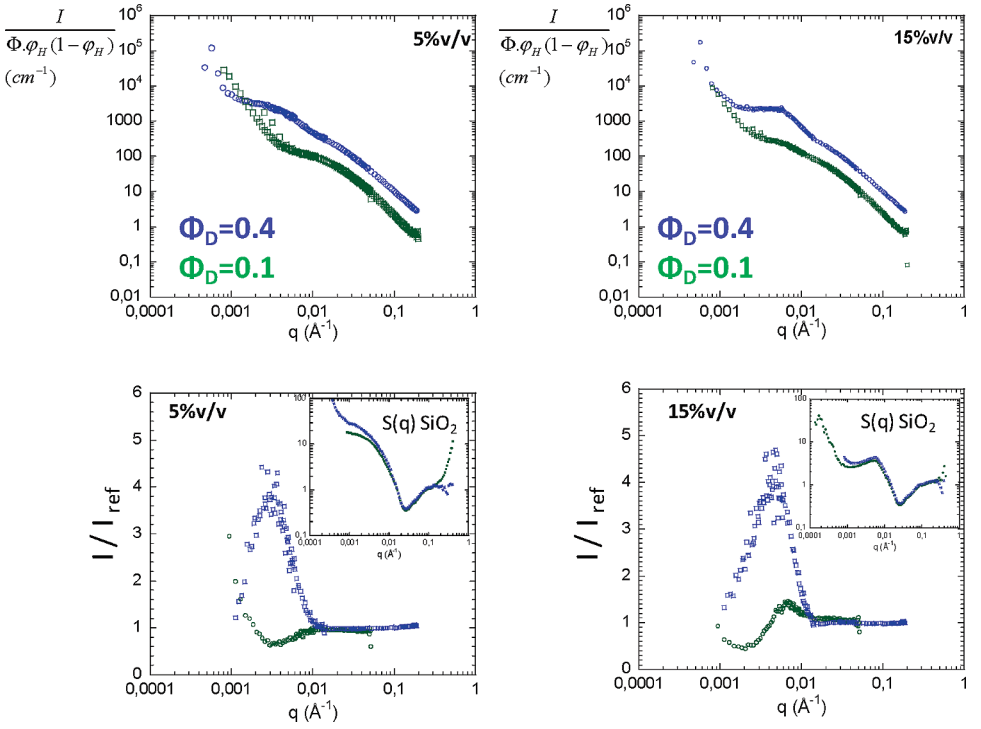

Figure 8. Comparison between three (blue curves) and four (green curves) components method: left, 5% v/v; right, 15% v/v for the molecular weight $M_w = 138\,000$ g·mol^{-1}. At the top are represented the scattering intensities obtained by SANS and the curves at the bottom the same scattering intensities normalized by the reference one to emphasize the "shoulder" effect. In the inset are shown the corresponding silica structure factors extracted from SAXS measurements.

q region of the data is again concerned by the scattering from crazes. We observe also in these data sets a shoulder, which increases when increasing the silica fractions. However, the amplitude of the shoulder seems to be reduced compared to the observations made with the three components methods.

III.2.4. Comparison between Three and Four Component Methods. Both approaches used in this work allow measurement of the chain conformation; in addition, the four component method allows one to check the perfect matching of silica. The main difference is related to the quantity of D-chains (or H-chains) involved in each method, which is $\Phi_D = 0.4$ for the three component method and $\Phi_D = 0.1$ for the four component one. Figure 8 shows for $M_w = 138$ kg mol^{-1} the comparison of the scattering intensity of 5% (left) and 15% (right) filled systems for the two methods (blue the three component and green the four component one) relative to $M_w = 138$ kg mol^{-1}. At intermediate and high q, the two methods lead to the same results: the scattering intensities are similar and superimpose well with the unfilled one. The fits using Debye equation give analogue value for the radius of gyration ($R_g = 105$ Å). The two methods clearly point to the same conclusion: the chain conformation is unaffected by the presence of fillers up to a typical size of the order of magnitude of the chain one. At larger scale some deviations are however observed. For 5% silica, the shoulder is not observed for the lower Φ_D value. This effect can be emphasized by dividing the scattering intensity of filled systems by the reference one (Figure 8 at the bottom). In this representation the peaks are clearly observed for $\Phi_D = 0.4$ and it is flatten for $\Phi_D = 0.1$. For 15% silica the shoulder is present, but clearly strongly reduced compared to $\Phi_D = 0.4$. The ratio of H-chains/D-chains appears therefore to be the key parameter for the presence of a shoulder in the low q regime.

IV. Discussion

The system proposed in this work displays a controlled and well-characterized filler spatial distribution which is a good model of many nanocomposites used, in particular, for reinforcement. It is well suitable to study the filler influence on chain spatial conformation, due also to the components, silica and polystyrene. The combination of SAXS measurements over a wide q range and TEM pictures provides a very clear view of silica arrangement in polymer matrix as a function of volume fraction. At low concentration (5% v/v), silica nanoparticles form small fractal aggregates with finite size which are not directly interconnected. At higher concentration, we determine exactly the typical size ξ characteristic of the connected network which is formed by the aggregates. The complementary TEM images highlight that the system remains homogeneous at larger scale.

The control of the structure at all scales made then consistent the use of very large q ranges in classical SANS, especially at low q. With such potential, it was particularly valuable to achieve a careful use of labeling and contrasts for SANS study of global chain conformation, using two different zero average contrast methods which validate the perfect matching of the silica. The most important result is that over a wide range of q, and molecular weights investigated, the chain conformation is not modified with respect to unfilled systems. This result was common to both experimental approaches employed. In spite of careful contrast matching, however, we observe unexpected extra-scattering in the low q region.

The scattering intensities of filled systems superimposes well with the reference ones in a q range from 0.008 to 0.2 Å^{-1} for all molecular weight and for the two labeling approaches. The data are well described by a classical chain Gaussian model with the same random walk parameters and the same radius of gyration than the one without silica. Fillers induce no change at the level of chain conformation in our PS-filled silica system. According to Mackay et al.,[23] chain swelling is expected when R_g of polymer is

larger than the nanoparticles radius. However, as previously explained, the direct comparison of our results within the existent literature[22−26] is not easily feasible because of the large variety of systems and filler dispersion, geometrical confinement, polymer filler interaction and sample processing methods. Sen et al.[25] have used similar Nissan nanoparticles in PS matrix, but with different solvent and casting method, which leads to a specific filler dispersion (coexistence of small aggregates and large agglomerates). In addition, their observations are affected by unperfected matching of the silica which induced the presence of an unclear peak at 0.04 $Å^{-1}$ independent of silica volume fraction. To our knowledge, in perfect matching conditions, this peak, which was only visible with SAXS investigations, is clearly related to the contact distance between primary silica nanoparticles inside aggregates. We believe that the observed unperturbed PS chain conformation is more general effect: it applies to an usual filled nanocomposite prepared by solvent casting, for various classical situations of filler dispersion: non connected finite size small aggregates and a connected filler network in our case, and larger aggregates and agglomerates as observed by Sen et al.[25] This non-modification of the chain conformation can be then correlated to a large range of dispersion qualities. Sample preparation methods could be a key parameter to explain the controversy results discussed above. It opens the discussion about expectable effects specific to these systems, namely chain adsorption, bridging[15] or dynamic (immobilized or bound layer[5]) induced by fillers. According to rheological investigations[32,38] and simulations,[15] these effects of indirect confinement are expected to take place at a scale which could be larger than the scale of direct geometrical confinement, for interfiller distances larger than the characteristic chain length (typically 10 nm). Indeed, the fraction of chains whose conformation or dynamic is affected by adsorption, bridging or interaction with fillers, is expected to influence the average resulting chain signal. Our results suggest that the fraction of affected chains is too low to be detected whatever the mass of the polymer chains, up to a characteristic length scale of 80 nm in the direct space (between 3 and 10 times the polymer chain size), even for high silica concentration.

The situation is not clear when considering larger distance, above 80 nm, accessible in the lower q domain (from 0.001 to 0.008 $Å^{-1}$). In this q-range, we can observe a shoulder which characteristics cannot be correlated in a systematic way with silica volume fractions, or with molecular weights of the polymer. This non reproducible phenomenon could have different origins. We can exclude immediately a first one, which would be the unperfected matching of the silica particles: we have clearly shown in this work with the four components method the perfect matching of the filler particles. In addition, we would expect this contribution to be similar for each of the samples which have been cast at the same time in the same conditions. This similarity is not observed: for a given molecular weight, 315 kg mol^{-1}, the shoulder is present at 15% v/v of silica and not at 5% v/v and inversely for 430 kg mol^{-1}. A possible explanation could be the influence of silica correlations on intrachains signal. Polymer chains can span filler over a range close to silica intercorrelations and "outline" the silica structure. The scattering intensity would be a convolution of filler structure factor and polymer chain form factors observed for polyelectrolyte chains in Vycor.[10] Note that in this case the scattering intensity showed changes at intermediate q: the chains appeared sensibly extended (×4) with a larger persistence length, and the scattering intensity becomes close to q^{-1} characteristic of a rod. This could be related with the cylindrical shape of the Vycor channels. The silica structure is different in our case, but anyhow we do not observe any signature of it at intermediate q. Third, the scattering shoulder could be due to an anomalous separation between the normal and the deuterated chains. This is supported by the fact that the amplitude of the

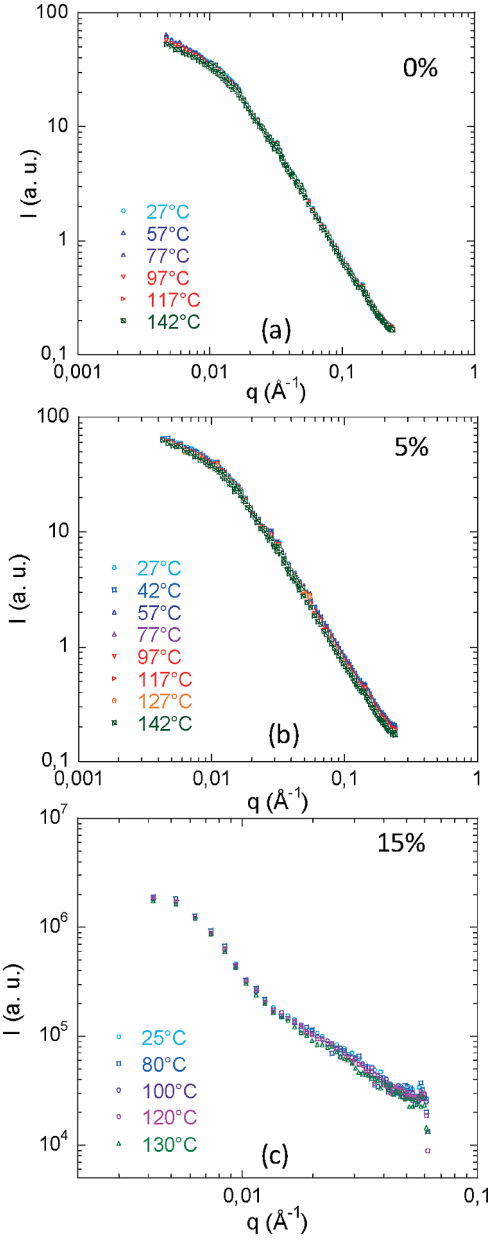

Figure 9. Effect of temperature on SANS intensity for the molecular weight M_w = 315 kg mol^{-1} for unfilled polymer (a), 5% v/v (b), and 15% v/v (c).

shoulder depends of the quantity of deuterated chains as showed with the two different methods of contrast variation (Figure 8). Moreover, the shape and the position of the shoulder in the filled samples are very similar to the signal measured for the larger mass reference sample (M_w = 1777 kg mol^{-1}), without silica in which normal and deuterated chains have indeed separated. This agrees with thermodynamics, which predict spinodal decomposition for such high degree of polymerization N of the polymer, due to the finite value of the Flory parameter χ_{HD} between normal and deuterated chains ($\chi_{HD}N\varphi_H\varphi_D > 1$,[9]). It is possible that the presence of the fillers triggers chain separation, by modification of the thermodynamic equilibrium conditions or by preferential adsorption of deuterated chains at the surface of the particles due to differences in surface tension. Phase separation between normal and deuterated species at the vicinity of a surface has already been studied for simple liquids[39] or polymer[40,41] and the decomposition amplitude can be controlled by the interaction strength between surface and polymer.[42] One weakness of such

explanation is that we observe a larger effect for the mass 315 kg mol^{-1} and the one of 430 kg mol^{-1}, while adsorption should not decrease with chain molecular weight. Similarly, spinodal decomposition should be more strongly triggered for larger mass. A possibility is that the vicinity of critical region (critical point) associated with spinodal decomposition could induce metastable conditions, leading to chain separation or not in an unsystematic way as a function of the polymer masses.

Since H chain/D chain separation, being an entropic process, is favored by temperature, we performed SANS measurements at higher temperature on chain conformation for molecular weight of 315 kg mol^{-1} filled with 0%, 5% and 15% v/v (Figure 9). As we mentioned before, for this molecular weight the shoulder is present at 15% v/v and not at 5% v/v. We observed complete superposition of the scattering intensities for all temperature range (from 27 to 142 °C) over the whole q range: the chain conformation is not modified by temperature, neither at 5% where the shoulder does not appear, nor at 15% v/v where the shoulder keeps the same amplitude for each temperature (Figure 9).

This is not in favor of processes related to phase separation,[43] and even less in favor of metastability as an explanation of our unsystematic observations. It remains possible that kinetic effects in the chain phase separations lead the systems in a blocked state where it is no longer sensitive to the temperature changes applied here.

V. Summary and Conclusion

We have investigated the polymer chain conformation in nanocomposites by SANS using the zero average contrast method. By this technique, we can properly match the silica scattering, so that the signal contains only the average form factor of the single chain in the presence of silica. We compare it with the one in the unfilled polymer bulk. Two experimental approaches have been studied and have provided the same results. In the same time we have performed SAXS measurements on the same samples for a good knowledge of the silica dispersion in the polymer matrix. In all cases the SANS signals superimpose well with the pure polymer ones in a large q range. Neither the molecular weights nor the silica volume fractions modify the chain form factor: the chain conformation is not affected by the presence of silica. We conclude that confinement and adsorption effects play a minor role on chain dimensions in a filler structure like the one of our system, carefully characterized, which is made of small aggregates. In the same time, our low q measurements make us observe extra scattering (shoulders) which are not clearly understood. This concerns larger scales than the one of the chain, while we expect that the inner chain conformation, measured at intermediate scale, is the most important since it acts on the mechanical properties. Such new results have the potential of better understanding of the reinforcement mechanisms[44] at the local scale.

Acknowledgment. The authors thank Chloé Chevigny for her helpful contribution to the H/D matrix synthesis.

References and Notes

(1) Heinrich, G.; Kluppel, M.; Vilgis, T. A. *Curr. Opin. Solid State Mater. Sci.* **2002**, *6*, 195–203.
(2) Medalia, A. I. *Rubber Chem. Technol.* **1986**, *59*, 432–454.
(3) Zou, H.; Wu, S.; Shen, J. *Chem. Rev.* **2008**, *108*, 3893–3957.
(4) Chabert, E.; Bornert, M.; Bourgeat-Lami, E.; Cavaillé, J.-Y.; Dendievel, R.; Gauthier, C.; Putaux, J. L.; Zaoui, A. *Mater. Sci. Eng. A* **2004**, *381*, 320–330.
(5) Berriot, J.; Montes, H.; Lequeux, F.; Long, D.; Sotta, P. *Macromolecules* **2002**, *35*, 9756–9762.
(6) Dutta, N. K.; Choudhury, N. R.; Haidar, B.; Vidal, A.; Donnet, J. B.; Delmotte, L.; Chazeau, J. M. *Polymer* **1994**, *35*, 4293–4299.
(7) Cotton, J.-P.; Decker, D.; Benoit, H.; Farnoux, B.; Higgins, J.; Jannink, G.; Ober, R.; Picot, C.; des Cloizeaux, J. *Macromolecules* **1974**, *7*, 863–872.
(8) Nierlich, M.; Williams, C. E.; Boué, F.; Cotton, J.-P.; Daoud, M.; Farnoux, B.; Jannink, G.; Pico, C.; Noan, M.; Wolff, C.; Rinaudo, M.; de Gennes, P. G. *J. Phys.* (*Paris*) **1979**, *40*, 701–704.
(9) De Gennes, P. G. *In scaling concepts in polymer physics*; Cornell University Press: Ithaca, NY, and London, 1979.
(10) Lal, J.; Sinha, S. K.; Auvray, L. *J. Phys. II* **1997**, *7*, 1597–1615.
(11) Nieh, M. P.; Kumar, S. K.; Ho, D. L.; Briber, R. M. *Macromolecules* **2002**, *35*, 6384–6391.
(12) Shin, K.; Obukhov, S.; Chen, J. T.; Huh, J.; Hwang, Y.; Mok, S.; Dobriyal, P.; Thiyagarajan, P.; Russell, T. P. *Nat. Mater.* **2007**, *6*, 961–965.
(13) Brûlet, A.; Boué, F.; Menelle, A.; Cotton, J.-P. *Macromolecules* **2000**, *33*, 997–1001.
(14) (a) Jones, R. L.; Kumar, S. K.; Ho, D. L.; Briber, R. M.; Russell, T. P. *Nature* **1999**, *400*, 146–149. (b) Jones, R. L.; Kumar, S. K.; Ho, D. L.; Briber, R. M.; Russell, T. P. *Macromolecules* **2001**, *34*, 559–567.
(15) Sarvestani, A. S. *Eur. Polym. J.* **2008**, *44*, 263–269.
(16) Mark, J. E.; Abou-Hussein, R.; Sen, T. Z.; Kloczkowski, A. *Polymer* **2005**, *46*, 8894–8904.
(17) Allegra, G.; Raos, G.; Vacatello, M. *Prog. Polym. Sci.* **2008**, *33*, 683–731.
(18) Sen, T. Z.; Sharas, M. A.; Mark, J. E.; Kloczkowski, A. *Polymer* **2005**, *46*, 7301–7308.
(19) Vacatello, M. *Macromolecules* **2001**, *34*, 1946–1952.
(20) Vacatello, M. *Macromolecules* **2002**, *35*, 8191–8193.
(21) Starr, F. W.; Schroder, T. B.; Glotzer, S. C. *Macromolecules* **2002**, *35*, 4481–4492.
(22) Nakatani, A. I.; Chen, W.; Schmidt, R. G.; Gordon, G. V.; Han, C. C. *Polymer* **2001**, *42*, 3713–3722.
(23) Mackay, M. E.; Tuteja, A.; Duxbury, P. M.; Hawker, C. J.; Van Horn, B.; Guan, Z.; Chen, G.; Krishnan, R. S. *Science* **2006**, *311*, 1740–1743.
(24) Botti, A.; Pyckhout-Hintzen, W.; Richter, D.; Urban, V.; Straube, E.; Kohlbrecher, J. *Polymer* **2003**, *44*, 7505–7512.
(25) Sen, S.; Xie, Y.; Kumar, S. K.; Yang, H.; Bansal, A.; Ho, D. L.; Hall, L.; Hooper, J. B.; Schweizer, K. S. *Phys. Rev. Lett.* **2007**, *98*, 128302.
(26) Tuteja, A.; Duxbury, P. M.; Mackay, M. E. *Phys. Rev. Lett.* **2008**, *100*, 077801.
(27) Bansal, A.; Yang, H.; Li, C.; Cho, K.; Benicewicz, B. C.; Kumar, S. K.; Schadler, L. S. *Nature materials* **2005**, *4*, 693.
(28) Sen, S.; Xie, Y.; Bansal, A.; Yang, H.; Cho, K.; Schadler, L. S.; Kumar, S. K. *Eur. Phys. J. Spec. Top.* **2007**, *141*, 161–165.
(29) Berriot, J.; Montes, H.; Martin, F.; Mauger, M.; Pyckhout-Hintzen, W.; Meier, G.; Frielinghaus, H. *Polymer* **2003**, *44*, 4909–4919.
(30) Nierlich, M.; Williams, C. E.; Boué, F.; Cotton, J.-P.; Daoud, M.; Farnoux, B.; Jannink, G.; Picot, C.; Noan, M.; Wolff, C.; Rinaudo, M.; de Gennes, P. G. *J. Phys.* (*Paris*) **1979**, *40*, 701–704.
(31) Chevigny, C.; Gigmes, D.; Bertin, D.; Jestin, J.; Boué, F. *Soft Matter* **2009**, *5*, 3741–3753.
(32) Jouault, N.; Vallat, P.; Dalmas, F.; Said, S.; Jestin, J.; Boué, F. *Macromolecules* **2009**, *42*, 2031–3040.
(33) Rivière, C.; Wilhelm, C.; Cousin, F.; Dupuis, V.; Gazeau, F.; Perzynski, R. *Eur. Phys. J. E.* **2007**, *22*, 1–10.
(34) Higgins, J. S.; Benoit, H. *Polymers and neutron scattering*; Oxford University Press: New York, 1994.
(35) Warner, M.; Higgins, J. S.; Carter, A. J. *Macromolecules* **1983**, *16*, 1931–1935.
(36) Bates, F. S. *Science* **1991**, *251*, 898–905.
(37) Mortensen, K.; Almdal, K.; Schwahn, D.; Bates, F. S. *J. Appl. Crystallogr.* **1997**, *30*, 702–707.
(38) Tsagaropoulos, G.; Eisenberg, A. *Macromolecules* **1995**, *28*, 6067–6077.
(39) Jestin, J.; Lee, L. T.; Privat, M.; Zalczer, G. *Eur. Phys. J. B* **2001**, *24*, 541–547.
(40) Jones, R. L.; Norton, L. J.; Kramer, E. J.; Bates, F. S.; Wiltzius, P. *Phys. Rev. Lett.* **1991**, *66*, 1326–1329.
(41) Geoghegan, M.; Nicolai, T.; Penfold, J.; Jones, R. A. L. *Macromolecules* **1997**, *30*, 4220–4227.
(42) Rysz, J.; Bernasik, A.; Ermer, H.; Budkowski, A.; Brenn, R.; Hashimoto, T.; Jedlinski, J. *Europhys. Lett.* **1997**, *40*, 503–508.
(43) Cabral, J. T.; Higgins, J. S.; Yerina, N. A.; Magonov, S. N. *Macromolecules* **2002**, *35*, 1941–1950.
(44) Jouault, N.; Dalmas, F.; Said, S.; Di Cola, E.; Schweins, R.; Jestin, J.; Boué, F. *Phys. Rev. E* **2010**, *82*, 031801.